Heat Transfer Characteristics of Porous Rocks: II. Thermal Conductivities of Unconsolidated Particles with Flowing Fluids

DAIZO KUNII and J. M. SMITH

Northwestern University, Evanston, Illinois

Experimental heat transfer studies were carried out in beds of unconsolidated glass beads and sand through which fluids were flowing. The scope of the measurements included four fluids, helium, air, carbon dioxide, and water liquid at atmospheric pressure in beds packed with four sizes of glass beads, 110, 370, 570, and 1,020 μ and with two sizes of sand, 110 and 240 μ. Flow rates ranged from 1 to 26 lb./(hr. sq.ft.) in a direction parallel and countercurrent to energy flow.

The data were interpreted in terms of apparent, effective thermal conductivities of the bed. The values of k_e increase significantly with mass velocity of fluid.

By considering the mechanism of heat transfer in porous media a relationship was developed between k_e and the heat transfer coefficient between fluid and particle. Treatment of the experimental data in this fashion, combined with available information for larger particles, results in a correlation of Nusselt and Reynolds numbers for air that covers the range $N_{Re_m} = 10^{-1}$ to 10^4.

There have been a number of heat transfer studies in beds of unconsolidated particles filled with stagnant fluids (*6, 10, 11, 12, 19, 20, 21, 22*). In a recent paper (*13*) Kunii and Smith reviewed these investigations and proposed equations for predicting stagnant conductivities for both unconsolidated sands and porous rocks. These equations take into account the effect of thermal and physical properties of the solid and fluid phases.

The problem of heat transfer with fluids flowing through the solid phase is not as far advanced as the stagnant case. Unsteady state measurements have been made (*3, 5, 16*) on beds of unconsolidated particles through which water is passed to displace the original fluid. Preston's (*3, 16*) original analysis neglected the effective thermal conductivity of the bed in the direction of flow and interpreted the data in terms of a heat transfer coefficient between solid particle and fluid. In a general paper Jenkins and Aronofsky (*9*) suggested that such longitudinal conductivities are significant for fine particles and low flow rates. Hadidi et al. (*5*) determined approximate values of k_e by comparing experimental temperature distributions in the bed with computed results. In a subsequent analysis Preston (*15*) neglected the limitation to heat transfer between solid and fluid and reported values of the effective thermal conductivity. Modification of his results to the form of plots of k_e vs. Reynolds number showed that the stagnant conductivity in the direction of flow may be increased two to three times when the fluid is in motion.

The objectives of the present work are the measurement of and the development of a method for predicting effective thermal conductivities parallel to the direction of flow in beds of unconsolidated particles. In particular it was desired to determine experimentally the effects of flow rate, particle size, and properties of the fluid phase on k_e. A mechanism of heat transfer has already been proposed (*13*) for beds of particles filled with stagnant fluid. Hence the extension of the theory that is needed is a description of the influence of the velocity of fluid through the bed.

EXPERIMENTAL WORK

The data for obtaining the effective thermal conductivity consisted of steady state measurements along the axis of a cylindrical bed of the particles. It was necessary to ensure that the only transfer of energy was parallel to the flow of fluid. To reduce transfer in the radial direction the bed was contained in a flask 2.54-in. I.D. and 5-in. length. As indicated in Figure 1 fluid was introduced into the top of the vertical bed and passed downwards countercurrent to the upward flow of energy as heat. Heating tape was wound around a copper cylinder below the bed, and energy was transferred through this copper cylinder, through which 5/16-in. diameter holes were drilled. To reach the bottom of the bed heat flowed upwards through the lower cylinder of copper into an upper cylinder drilled with 3/16-in. holes and finally through a bed of lead shot. The upper copper cylinder, drilled with smaller holes for the fluid and surmounted with lead shot, was used to obtain a uniform temperature across the tube diameter at the bottom of the bed.

The flask was enclosed in a steel casing equipped with flanges at both ends. Leakage of fluid between the flask and the casing was prevented by plugging the annular spaces with sealing cement. Temperatures were measured with one set of copper-constantan thermocouples (30 B and S gauge) located along the central axis of the bed and a second set near the tube wall, as shown in Figure 1. The fluid entered the top of the apparatus at slightly below room temperature. The heat input was adjusted to provide a longitudinal temperature variation in the bed as large as conveniently possible, and of the order of 200°F. Temperature control was achieved with a thermocouple embedded in the top of the lower copper cylinder. During a run the reading of this thermocouple was maintained constant at a level between 300° and 500°F., depending upon the flow rate of fluid through the bed.

To obtain near adiabatic operation in the radial direction cooling coils were wound around the steel casing as illustrated in Figure 1. It was necessary to provide cooling because heat flowed from the heated section upwards through the copper cylinders and steel casing. By adjustment of the water rate through the coils it was possible to maintain essentially identical readings of the thermocouples at the axis and edge of the bed, thus providing the condition for no flow of heat in the radial direction. Temperatures were observed to 0.5°F. by a recorder. The flow rates of the gases through the bed were measured with a wet-test meter and the water rate determined by direct volumetric measurement.

SCOPE OF DATA

Measurements were made on beds packed with four different sizes of glass beads with five fluids, helium, nitrogen, air, carbon dioxide, and liquid water. The characteristics of the beds of particles are:

glass beads	1,020 μ (0.0402 in.), void fraction = 0.39
	570 μ (0.0224 in.), void fraction = 0.37
	370 μ (0.0146 in.), void fraction = 0.37
	110 μ (0.0043 in.), void fraction = 0.34
sand	240 μ (0.0095 in.), void fraction = 0.44
	110 μ (0.0043 in.), void fraction = 0.40

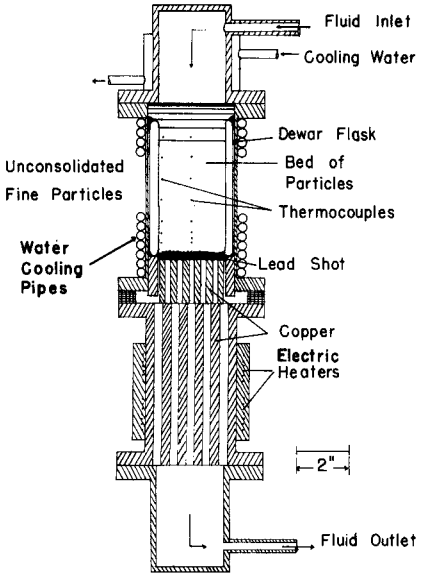

Fig. 1. Outline of experimental equipment.

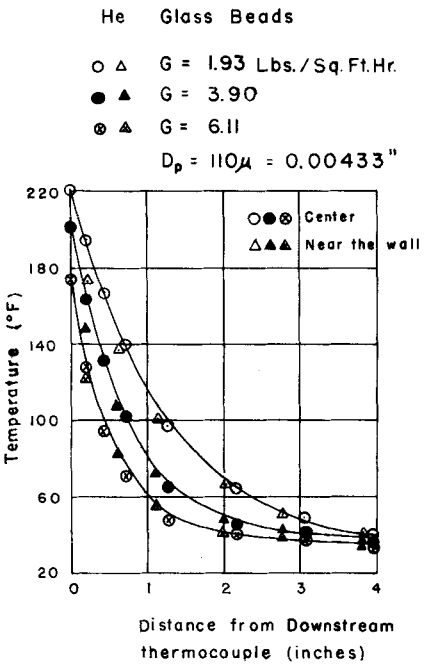

Fig. 2. Examples of temperature distribution in packed bed of fine particles.

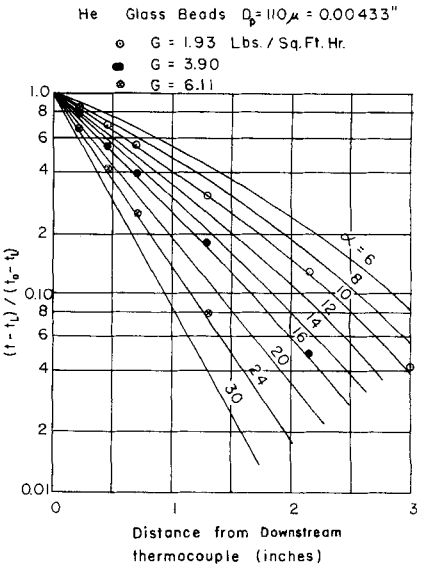

Fig. 3. Dimensionless temperature distribution.

The flow rates of interest in beds of fine particles are relatively low. In this study the mass velocities were from 1 to 26 lb./hr. sq. ft. of total area, and the corresponding modified Reynolds numbers ranged from 1 x 10^{-3} to 1. All the data were taken at atmospheric pressure, as measured at the exit of the lower copper cylinder (Figure 1).

RESULTS

The method of measurement did not provide information on the small, but finite, temperature difference between the fluid and the particles. Hence the data were analyzed to obtain apparent values for the thermal conductivity of the heterogeneous system. This procedure is based on the concept that the system possesses a single, mean temperature at any point in the bed. The resultant values of k_e thus include the effect of heat transfer between fluid and solid particles. With this model, and neglecting the heat transfer in the radial direction, one can relate the effective thermal conductivity to the temperature profile by

$$G C_p \frac{d\bar{t}}{dx} = -k_e \frac{d^2t}{dx^2} \qquad (1)$$

With the boundary conditions

$$x = 0 \qquad t = \bar{t}_o$$
$$x = L \qquad t = \bar{t}_L \qquad (2)$$

the solution of Equation (1) is

$$\frac{\bar{t} - \bar{t}_L}{\bar{t}_o - \bar{t}_L} = 1 - \frac{1 - e^{-\alpha x}}{1 - e^{-\alpha L}} \qquad (3)$$

$$\alpha = G C_p / k_e \qquad (4)$$

Equation (3) was used to evaluate α by utilizing the measured temperature profile.

Figure 2 illustrates the temperature vs. distance relationship observed. Three examples are given showing the effect of mass velocity on the shape of the profile. Included on the figure are the temperature measurements at both the axis and wall positions. Data were taken at too few axial distances (8 locations) to permit gainful application of a statistical technique. In lieu of this curves were prepared showing the relationship between temperature and distance, x, as required by Equation (3). These curves could be drawn after two experimental points were used to fix numerically the boundary conditions [Equations (2)]. Figure 3 illustrates the resultant curves for the runs shown in Figure 2, with $x = 0$ chosen at the lowest thermocouple location and $L = 3.75$ in. Superimposing the calculated curves from Figure 3 on the experimental profiles plotted in Figure 2 one can evaluate an average value of α for each run. The data points from Figure 2 are shown also on Figure 3 to illustrate the results. For these selected runs values of α are noted to be approximately 10, 16, and 24.

From α the effective thermal conductivity was determined by the use of Equation (4) and a mean specific heat for the fluid in the bed. The results for all the runs are shown in Figures 4 to 8 for the four fluids*. A mean value of the viscosity was employed in computing the modified Reynolds numbers. Since the properties change slowly with temperature at atmospheric pressure, errors introduced in using mean properties are less than the uncertainties due to the temperature and location measurements.

The greatest errors in the determination of k_e probably arose from the in-

* Copies of tables of the experimental data are available in the Chemical Engineering Department, Northwestern University, Evanston, Illinois.

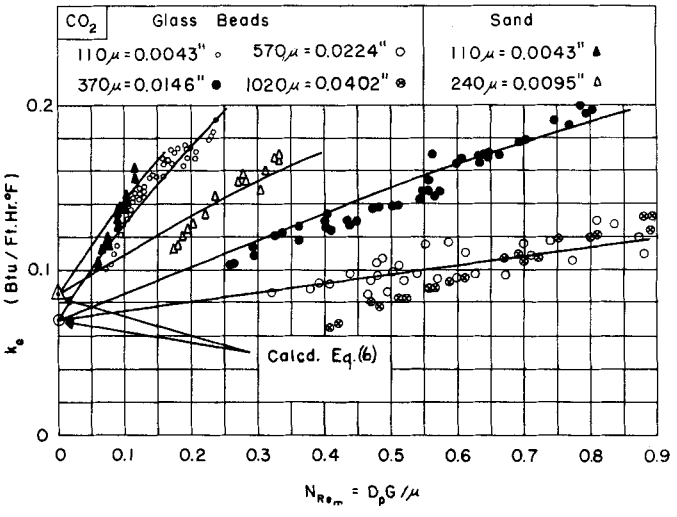

Fig. 4. Data for carbon dioxide.

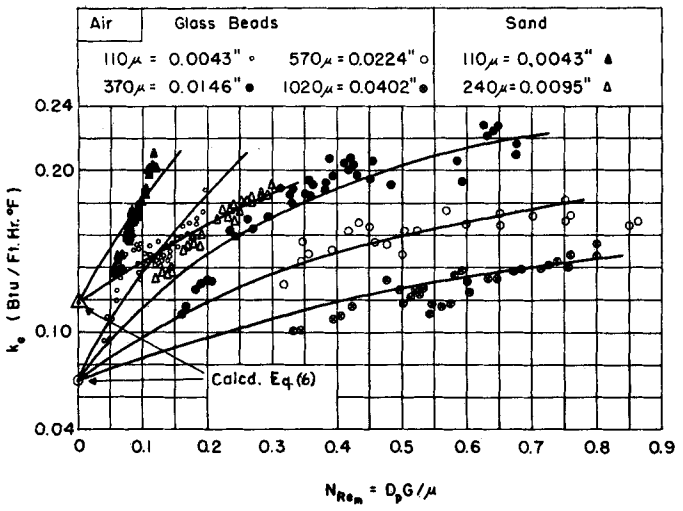

Fig. 5. Data for air.

accuracy in measuring the location of the thermocouples in the bed and from fluctuations in flow rate, particularly at low values. Less significant uncertainties include errors in temperature measurements and deviation from adiabatic operation and steady state operation.

The points for the stagnant conductivity, shown on Figures 4 to 8, were computed from the following equations derived in the earlier paper (*13*):

$$\phi = \phi_2 + (\phi_1 - \phi_2)\frac{\epsilon - 0.260}{0.216} \quad (5)$$

$$\frac{k_e^\circ}{k_g} = \epsilon + \frac{0.9\,(1-\epsilon)}{\phi + \frac{2}{3}\,(k_g/k_s)} \quad (6)$$

In the application of these expressions the thermal conductivity of the beads was first computed from the assumed composition of the glass (36.2 wt. % silicon dioxide, 6.7% zinc oxide, 7.7% boron trioxide, 3.5% aluminum oxides, 44.5% barium oxide, 0.2% potassium oxide, 0.2% calcium oxide, 0.3% antimony trioxide, and 0.7% arsenic pentoxide), with published information (*8*) used. The result was $k_s = 0.47$ B.t.u./(ft. hr. °F.). This value, applicable at 77°F., was assumed to be satisfactory also at the mean bed temperature, which was always close to 100°F. For sands a value of $k_s = 2.7$ was chosen. This is the mean of the thermal conductivities for quartz and vitreous silica.

The stagnant conductivities so evaluated are shown in Figures 4 to 8 at zero Reynolds number. These values are helpful in locating the lower ends of the curves, because accurate values for k_e are difficult to measure at low flow rates.

APPARENT CONDUCTIVITIES AND HEAT TRANSFER BETWEEN PARTICLES AND FLUID

It was mentioned that the apparent, effective conductivities as measured in this study include the effect of heat transfer between solid particles and the fluid stream. This is because the thermocouples in the bed indicated neither fluid nor gas temperatures but values between the two. The mechanism of energy flow in the experiments consisted of transfer through the solid particles upwards in the bed and transfer from the particles out into the fluid phase. At steady state conditions the temperature of the particles will be somewhat above that (t_g) of the fluid, although the difference will be small. With this concept of heat exchange in the bed (*4, 23*) it is possible to relate the apparent effective conductivity and the heat transfer coefficient between the solid and fluid. This relationship is developed in the following paragraphs.

For the system used in this investigation, with parallel but countercurrent flow of heat and fluid, energy balances on the fluid and solid phases give the expressions

$$\epsilon\, k_g \frac{d^2t_g}{dx^2} + G\,C_p\frac{dt_g}{dx} = -\,h\,a\,(t_s - t_g) \quad (7)$$

$$k_e^* \frac{d^2t_s}{dx^2} = h\,a\,(t_s - t_g) \quad (8)$$

In reference *13* equations were developed for k_e° by adding the contributions due to heat flow through the solid phase and through the voids. The quantity k_e^* represents the solid-phase contribution to the stagnant conductivity. Therefore at low temperatures where radiation is unimportant, k_e^* is given by the second term on the right side of Equation (6); hence

$$k_e^* = k_g \frac{0.9\,(1-\epsilon)}{\phi + 2/3\,(k_g/k_s)} \quad (9)$$

Equations (7) and (8) can be simplified by elimination of t_s and by introducing Reynolds, Prandtl, and Nusselt numbers, as defined in the notation. The surface area per unit volume of packed bed can be approximated by assuming that the particles are spherical and that their entire surface is effective for heat transfer. Under these conditions this is given by

$$a = \frac{6\,(1-\epsilon)}{D_p} \quad (10)$$

Carrying out these operations one can reduce Equations (7) and (8) to

$$D_p^4\frac{d^4t_g}{dx^4} + \frac{N_{Pr}N_{Re}}{\epsilon}D_p^3\frac{d^3t_g}{dx^3} - 6\,(1-\epsilon)\left(\frac{1}{\epsilon} + \frac{k_g}{k_e^*}\right)N_{Nu}\,D_p^2\frac{d^2t_g}{dx^2} - 6\frac{(1-\epsilon)}{\epsilon}$$

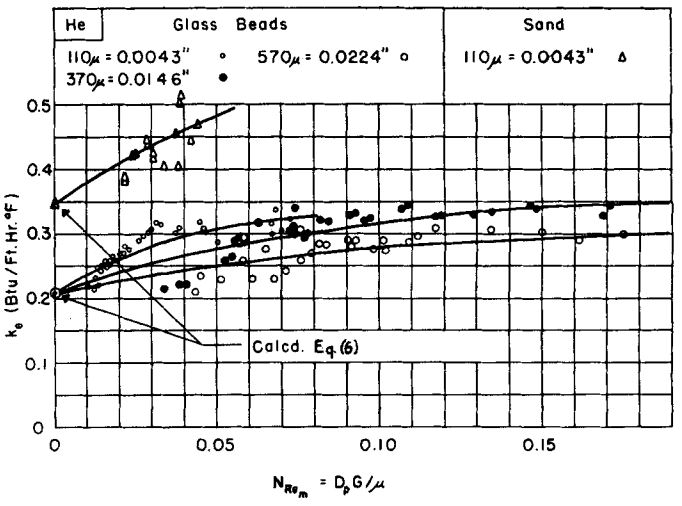

Fig. 6. Data for helium.

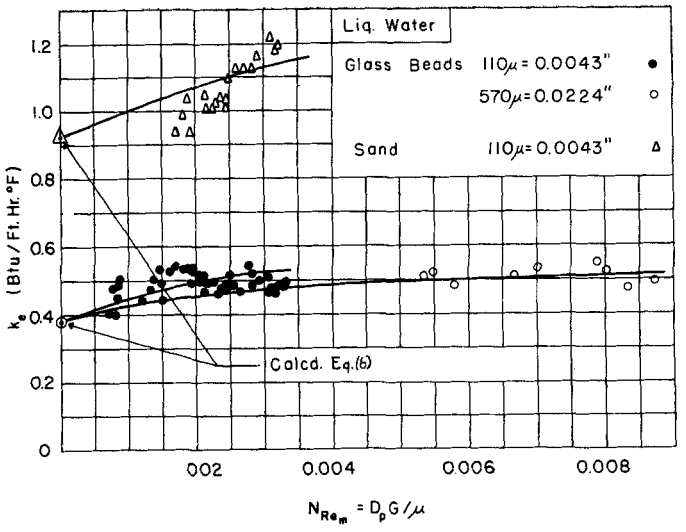

Fig 7. Data for liquid water.

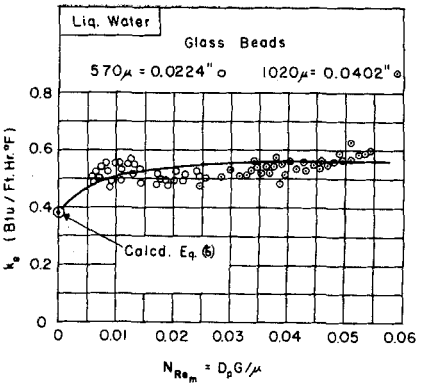

Fig. 8. Data for liquid water.

$$\left(\frac{k_g}{k_e^*} N_{Pr} N_{Re_m} N_{Nu} D_p\right) \frac{dt_g}{dx} = 0 \quad (11)$$

The temperature difference between the fluid and adjacent solid particle, $t_g - t_s$, is too small to be determined accurately for beds of fine particles (23). The temperature profiles in the solid and fluid phases must be on either side of, and very close to, the measured profile illustrated in Figure 2. Therefore for beds of fine particles the mean-temperature ratio defined by Equation (3) is nearly the same as the ratio expressed in terms of t_g; that is Equation (3) may be written as

$$\frac{t_g - t_{g_L}}{t_{g_o} - t_{g_L}} = \frac{\bar{t} - \bar{t}_L}{\bar{t}_o - t_L} = 1 - \frac{1 - e^{-a\alpha}}{1 - e^{-aL}} \quad (12)$$

Equation (12) can be used to formulate the derivatives in Equation (11) in terms of α. Carrying out this operation and expressing α in terms of k_e [Equation (4)] one can transform Equation (11) to

$$\left(\frac{k_e}{k_e^*}\right)^3 - \left(1 + \frac{\epsilon k_g}{k_e^*}\right)\left(\frac{k_e}{k_e^*}\right)^2 - \frac{N^2_{Pr} N^2_{Re_m}}{6(1-\epsilon) N_{Nu}}\left(\frac{k_g}{k_e^*}\right)\left(\frac{k_e}{k_e^*}\right) + \frac{N^2_{Pr} N^2_{Re_m}\,\epsilon}{6(1-\epsilon) N_{Nu}}\left(\frac{k_g}{k_e^*}\right)^2 = 0 \quad (13)$$

This equation provides the desired relationship between the apparent conductivity and the heat transfer coefficient (in the form of Nu). When one solves Equation (13) for the Nusselt number

$$N_{Nu} = \frac{N^2_{Pr} N^2_{Re_m}}{6(1-\epsilon)} \frac{1 - \frac{\epsilon k_g}{k_e}}{\left(\frac{k_e}{k_g}\right)\left[\frac{k_e}{k_e^*}\left(1 - \frac{\epsilon k_g}{k_e}\right) - 1\right]} \quad (14)$$

This expression can be used to evaluate the heat transfer between particle and fluid from data for the apparent, effective conductivity. Also the relationship can be adopted to predict apparent, effective conductivities from a knowledge of the heat transfer coefficient between particle and fluid. As Equation (13) suggests, this requires the solution of a cubic equation. The smallest positive root is the desired value for k_e/k_e^*.

If the fluid has a comparatively low thermal conductivity, for example gases such as air or carbon dioxide, $\epsilon k_g/k_e$ is much smaller than unity. For these fluids Equation (14) simplifies to a quadratic form whose solution is

$$\frac{k_e}{k_e^*} = \frac{1}{2}\left[1 + \left(1 + \frac{2}{3(1-\epsilon)} \frac{N^2_{Pr} N^2_{Re_m}}{(k_e^*/k_g) N_{Nu}}\right)^{1/2}\right] \quad (15)$$

DISCUSSION ON PREDICTION OF APPARENT, EFFECTIVE CONDUCTIVITIES

There are available a number of studies of heat transfer coefficients be-

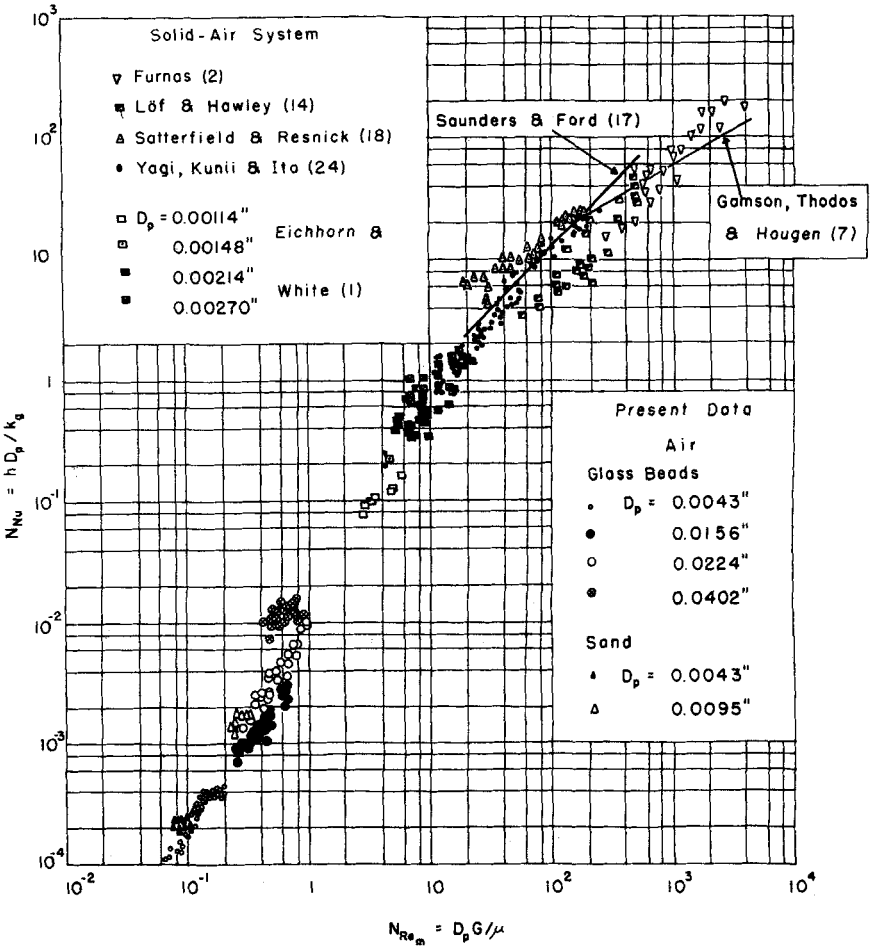

Fig. 9. Nusselt vs. Reynolds number for air in packed beds.

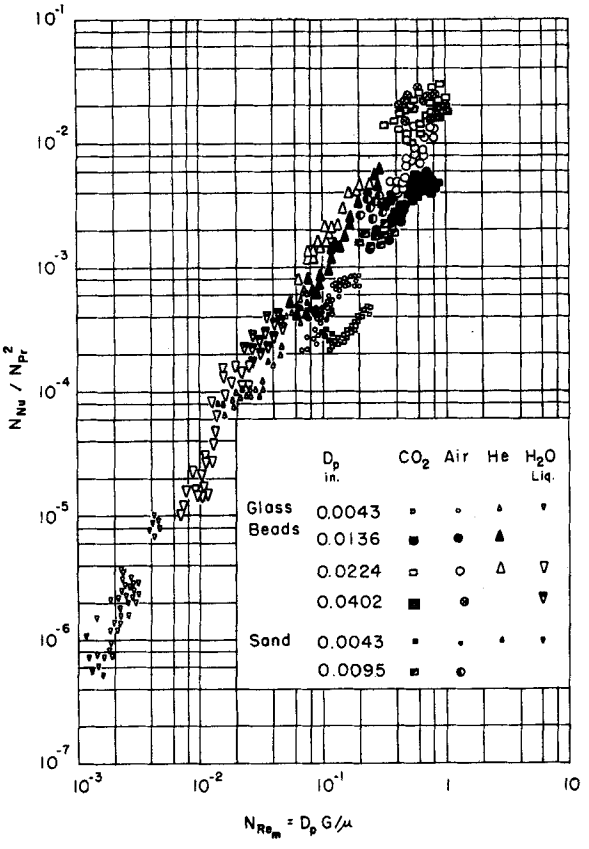

Fig. 10. Nusselt vs. Reynolds number for different fluids.

tween fluid and solid particles in packed beds. Table 1 summarizes the conditions used for a series of these studies covering a range of particle sizes. All the data are for air flowing through the bed. Figure 9 shows a plot of these results in the form of Nusselt vs. modified Reynolds numbers. The data for the present study on smaller particles can be estimated on the same basis by evaluating Nusselt numbers from Equation (14). The calculations were carried out by using the experimental results for k_e illustrated in Figure 5. The values of k_e^* were determined from Equation (9) as described in reference *13*. The application of Equation (14) is subject to errors when k_e/k_e^* is near unity; this is likely to occur at very low flow rates. Despite the scatter in some of the data points. Figure 9 indicates consistency between the previously published results at high Reynolds numbers and the present data at considerably lower values of N_{Re_m}. The data for the small glass beads and sand particles (Figure 9) show a distinct effect of particle size; the Nusselt number increases with increasing particle diameter. Additional data covering a wider range of sizes are needed to determine completely the effect of particle diameter.

Figure 10 shows plots of N_{Nu}/N^2_{Pr} vs. N_{Re_m} for all four fluids studied. This method of plotting, as suggested by Equation (14), tends to bring the data for different fluids together. Complete coincidence of the results for various fluids is not expected in Figure 10 because k_e/k_g and k_e/k_e^* are dependent, to some extent at least, on k_g and the Reynolds number. As in Figure 9 data for different particle sizes would not fall on the same curve in Figure 10.

Figure 10 and Equation (13) suggest an approximate method of predicting the apparent, effective thermal conductivity of a bed of unconsolidated particles, for the sizes investigated, and through which helium, air, carbon dioxide, or water is flowing. The procedure is as follows: From the nature of the fluid, the particle size, and the flow rate estimate the Nusselt number from Figure 10. Then evaluate k_e^* from Equation (9) and k_e from Equation (13). It may be observed that the ratio k_e/k_e^* computed from Equation (13) is a measure, in part, of the effect of flow on the stagnant conductivity. It is not solely a measure of this effect to the extent that k_e° differs from k_e^*. This difference is larger for fluids of comparatively high thermal conductivity, such as water. As data are accumulated on Nusselt number vs. Reynolds number, it is expected that the approximate Figure 10 can be developed into an accurate method of predicting the heat transfer coefficient in beds of small particles.

It should be emphasized that the results presented apply only for heat transfer parallel to the flow of fluid. It is expected that apparent conductivities in the radial direction would be appreciably different.

Table 1. Experimental Conditions for Heat Transfer Coefficients Between Solid Particles and Fluids in Packed Beds

Reference	Fluid	Type of particle	Particle size
Furnas (*2*)	Air	Iron, iron oxide balls	0.32 to 1.5 in.
Löf and Hawley (*14*)	Air	Granite (granular)	4 mesh to 1.5 in.
Satterfield and Resnick (*18*)	H_2O_2-H_2O	Catalytic metal spheres	0.20 in.
Yagi, Kunii, and Ito (*24*)	Air	Steel balls, glass beads, lead shot	0.019 to 0.197 in.
Eichorn and White (*1*)	Air	Plastic spheres	24/28 mesh to 150/180 mesh
Hougen, Gamson, and Thodos (*7*)	Air	Cellite particles	0.161 to 0.456 in.

ACKNOWLEDGMENT

The assistance of the California Research Corporation (Standard Oil Company of California) and the Petroleum Research Fund (American Chemical Society) by providing financial grants for this work are acknowledged. R. S. Rosler assisted in obtaining some of the experimental data.

NOTATION

a = surface area of spherical particles per unit volume of packed bed, sq. ft./cu. ft.
C_p = specific heat at constant pressure, B.t.u./(lb. °F.)
D_p = diameter of spherical particles, ft.
G = mass velocity of fluid through the bed, lb./(hr.)(sq. ft. of total cross-sectional area of bed)
h = heat transfer coefficient between solid particle and fluid phase, B.t.u./(hr. sq. ft. °F.)
k_e = apparent, effective thermal conductivity of the bed with

flowing fluid, B.t.u./(hr. ft. °F.)

k_e° = stagnant effective thermal conductivity of bed (that is bed filled with stationary fluid), B.t.u./(hr. ft. °F.)

k_e^q = effective thermal conductivity representing heat transfer through the solid particles, B.t.u./(hr. ft. °F.)

k_g = thermal conductivity of fluid in bed, B.t.u./(hr. ft. °F.)

k_s = thermal conductivity of solid particles in bed, B.t.u./(hr. ft. °F.)

L = distance between extreme thermocouples at the axis of the bed, ft.

N_{Nu} = Nusselt number, $h\,D_p/k_g$, dimensionless

N_{Pr} = Prandtl number, $C_p\,\eta/k_g$, dimensionless

N_{Re_m} = modified Reynolds number, $D_p\,G/\eta$, dimensionless

t = temperature, °F., $\overline{t}$ denotes mean temperature in bed as indicated by thermocouple readings

x = distance measured from downstream thermocouple in the bed, ft.

Subscripts

g = fluid phase

s = solid phase

o = position at downstream thermocouple in the bed

L = position at a distance L from downstream thermocouple

Greek Letters

α = $G\,C_p/k_e$, ft.$^{-1}$

ϵ = void fraction in the bed

ϕ = parameter measuring the heat transfer resistance in the stagnant fluid adjacent to the contact point of adjacent solid particles, dimensionless; ϕ_1 and ϕ_2 refer to the loose and dense packing arrangements for spherical particles (*13*)

η = viscosity of fluid, lb./(hr. ft.)

LITERATURE CITED

1. Eichhorn, J. W., and R. R. White, *Chem. Eng. Progr. Symposium Series No. 4*, **48**, 11 (1952).
2. Furnas, C. C., *Ind. Eng. Chem.*, **22**, 26 (1930); *Bull. U.S. Bureau Mines*, No. 361 (1932).
3. Greenstein, R. I., and F. W. Preston, *Producers Monthly*, **17**, No. 16 (1953).
4. Grootenhuis, P., R. C. A. Mackworth, and O. A. Saunders, "Proceedings of General Discussion on Heat Transfer," p. 363, Inst. Mech Engrs. (London) (1951).
5. Hadidi, T. A. R., R. F. Nielson, and J. C. Calhoon, *Producers Monthly*, **20**, No. 16 (1956).
6. Harbert, W. D., D. C. Cain, and R. L. Huntington, *Ind. Eng. Chem.*, 33, 257 (1941).
7. Hougen, O. A., B. W. Gamson, and George Thodos, *Trans. Am. Inst. Chem. Engrs.*, **39**, 1 (1943).
8. "International Critical Tables," Vol. 5, p. 230.
9. Jenkins, R., and J. D. Aronofsky, 18th Technical Conference on Petroleum, Mineral Industries Experiment Station Bulletin No. 64, p. 69, The Pennsylvania State University (1954).
10. Kannuluick, W. G., F. K. Scholar, and L. H. Martin, *Proc. Roy. Soc. (London)*, **141A**, 144 (1933).
11. Kimura, M., *Chem. Eng. (Japan)*, **21**, 472 (1957).
12. Kling, G., *Forsch. Gebiete Ingenieurw.*, **9**, 28, 82 (1938).
13. Kunii, Daizo, and J. M. Smith, *A.I.Ch.E. Journal*, **6**, 71 (1960).
14. Löf, G. O. G., and R. W. Hawley, *Ind. Eng. Chem.*, **40**, 1061 (1948).
15. Preston, F. W., Ph.D. thesis, Pennsylvania State Univ., State College, Pennsylvania (June, 1957).
16. ———, and R. D. Hazen, *Producers Monthly*, **18**, No. 44 (1954).
17. Saunders, O. A., and H. Ford, *Journal Iron Steel Institute*, **141**, 291 (1940).
18. Satterfield, C. N., and Hyman Resnick, *Chem. Eng. Progr.*, **50**, 504 (1954).
19. Schumann, T. E. W., and V. Voss, *Fuel*, **13**, 249 (1934).
20. Waddams, A. L., *J. Soc. Chem. Ind.*, **63**, 337 (1944); *Chem. and Industry*, 206 (1944).
21. Weininger, J. L., and W. C. Schneider, *Ind. Eng. Chem.*, **43**, 1229 (1951).
22. Yagi, Sakae, and Daizo Kunii, *A.I.Ch.E. Journal*, 3, 373 (1957).
23. ———, and Noriaki Wakao, *A.I.Ch.E. Journal*, **6**, No. 4, (1960).
24. Yagi, Sakae, Daizo Kunii, and K. Ito, unpublished paper.

Manuscript received March 21, 1960; revision received May 25, 1960; paper accepted May 27, 1960. Paper presented at A.I.Ch.E. Mexico City meeting.

A Quantitative Treatment of the Forgotten Effect in Liquid Thermal Diffusion

JOHN D. BALDESCHWIELER

Harvard University, Cambridge, Massachusetts

The influence of the concentration gradient on the density gradient in a thermal-diffusion column is called the *forgotten effect*. A modification of the theory developed by Furry, Jones, and Onsager is proposed to include the effect of the horizontal concentration gradient. A sample calculation with the system toluene-cyclohexane shows that the equations predict the proper behavior for a forgotten-effect system.

In quantitative treatments of thermal diffusion column operation it is frequently assumed that the horizontal density gradient in a column $\partial\rho/\partial x$ is caused only by the horizontal temperature gradient (*1*, 2, 3); that is

$$\frac{\partial \rho}{\partial x} = \left(\frac{\partial \rho}{\partial T}\right)\left(\frac{\partial T}{\partial x}\right) \qquad (1)$$

However $\partial\rho/\partial x$ must also depend on the horizontal gradient in composition of the mixture in the column. The composition gradient arises from the separation of the mixture by thermal diffusion. The influence of the concentration gradient on the density gradient in a column has been called the *forgotten effect* (*4*). The horizontal density